MIJST
MIST International Journal of Science and Technology

Effect of Heat Input on the Wire-Arc Additive Manufactured Steel Structures

Vishal Kumar[1] and Amitava Mandal[2*]

Department of Mechanical Engineering, Indian Institute of Technology (Indian School of Mines), Dhanbad, India

emails: [1]*vishal0101kumar@gmail.com; and* *[2]*amitava03@gmail.com*

ARTICLE INFO

Article History:

Received: 05th April 2023
Revised: 14th May 2023
Accepted: 16th May 2023
Published: 25th June 2023

Keywords:

Metal Additive Manufacturing
Directed Energy Deposition
Heat Input
WAAM

ABSTRACT

Wire arc additive manufacturing (WAAM) is one of the less-explored metal 3D printing technologies that hold up a huge potential for large-scale product manufacturing across multiple industries. The low-cost AM uses arc energy as a heat source and metallic wire as a feedstock material. The process is sustainable and supports green manufacturing. However, the major challenge associated with the WAAM is that heat management leads to the development of residual stress causing dimensional inaccuracy and poor surface finish. Therefore, four-layer straight wall structures are fabricated by depositing material layer-upon-layer with nine distinct heat inputs (HI). The prime focus of the work is to study the effect of HI on the dimensional accuracy and the quality of deposited structures. The influence of deposition height on the surface topography is investigated. Furthermore, the effect of HI on the mechanical properties of the WAAM-printed thin wall is examined. The results show that with increase in the number of depositing layers, surface roughness values get increased under the similar process parameter used for the part fabrication. Therefore, it is recommended to re-adjust the process parameter after certain layers of deposition with proper monitoring of the thermal condition in the deposited layers while fabricating medium to large WAAM components. The outcomes from the studies show that increases in the HI while fabricating the WAAM component deteriorates the surface quality of the deposited layer and are responsible for reducing the mechanical properties of the WAAM-printed component.

1. INTRODUCTION

Wire and arc additive manufacturing (WAAM) is a revolutionary process classified under directed energy deposition (DED) that utilizes the combination of metallic wire as a feeding material and arc heat energy as a heat source to fabricate structures by depositing materials layer upon layer (Kumar *et al.*, 2021). The welding-based additive manufacturing (AM) has exceptional application potential in marine ships, aerospace, automobiles, petrochemical, nuclear power, and many other industries that serve the dual purposes of manufacturing and remanufacturing the components (Hideaki *et al.*, 2020). The manufacturing method offers several advantages over traditional manufacturing such as high flexibility, high energy efficient process, integral forming, sustainable manufacturing, low capital cost, low buy-to-fly (BTF) ratio, and short manufacturing lead time (Gisario *et al.*, 2019). The repeated heat cycle during material deposition and the discrete-stacking principle is liable to generate thermal stresses and metallurgical defects in the parts fabricated via WAAM (Zeng *et al.*, 2021). The surface quality and dimensional accuracy of the structure built strongly depend on the fabrication process parameters that ultimately determine the molten pool size, temperature, and molten metal viscosity. These WAAM process parameters, in combination with heat dissipation conditions, determine the rate of solidification, grain size, and orientation that impact the morphological evolution and mechanical strength of the built structure (Filippov *et al.*, 2021). Besides several limitations, the low-cost WAAM manufacturing technique remains most suited for printing large-scale components because of better material utilization and a high material deposition rate compared to other metal additive manufacturing. In the area of improving the quality of WAAM fabricated component studies have been carried out by researchers in different domains. Wang *et al.* investigated the influence of heat input

on the microstructure and mechanical properties of the WAAM-deposited Al-Cu-Sn alloy. The authors observed an increase in the size and number of pores within the deposited alloy leading to reduce its mechanical strength (Wang *et al.*, 2020) Another researcher studied the impact of preheating the base plate and cooling the substrate plate on the geometry of the deposited weld bead using the WAAM process (Gudur *et al.*, 2021). Zhou *et al.* performed several experiments to optimize the process parameter to reduce heat input to the WAAM process and improved the surface quality of the fabricated part (Zhou *et al.*, 2020). To minimize problems of residual stress in the WAAM-built part researchers used the roll pressure technique while fabricating parts that not only refine the grain structure but also reduce the geometric distortion and control the residual stress (Hönnige *et al.*, 2018). Furthermore, the effect of temperature on the mechanical properties of the fabricated aluminum alloy has been investigated, and results show an improvement in the micro-hardness and tensile properties of the built specimen when the built specimen undergoes the solution treatment and natural aging (Zewu *et al.*, 2018). Guo *et al.* investigated the effect of heat treatment on the microstructure and mechanical properties of the WAAM fabricated wall structures. The application of heat treatment improves tensile strength and ductility and reduces the mechanical anisotropy along the vertical and horizontal direction of the fabricated wall (Guo *et al.*, 2022). On the other side, the researcher worked to rectify one of the major problems of surface waviness restricting the economical use of the as-deposited WAAM component. The concept of side rolling of the deposited layers at room temperature while fabricating the structure has been introduced which lowered the surface waviness and also improved the strength due to work hardening (Dirisu *et al.*, 2020). Xiong *et al.* studied the effect of process parameters on the quality of deposited structure (Xiong *et al.*, 2018). They observed that by maintaining a constant ratio of wire feed speed and travel speed, the surface roughness increased with the increase of wire feed rate. Thus, the WFR was found to be the major influential parameter deciding the forming appearance of thin wall WAAM components.

Critical analysis of the literature sources is mostly devoted to the investigation of process parameters in correlation to their micro-structural changes and mechanical behaviour of the WAAM fabricated part. Therefore, as per the author's best knowledge study based on the effect of heat input on the surface topography, surface quality and mechanical properties of the WAAM printed components have been the least explored research areas in this domain. Therefore, the objective of the work is to fabricate four-layer straight wall structures at nine different heat inputs. The extracted sample was further used to study the impact of heat input on the surface quality of the printed wall along the deposition direction by calculating average surface roughness values using the roughness tester and surface waviness of the deposited layers using the non-contact optical profilometer. The study continued with investigating the impact of heat input on the mechanical properties of the built wall structures and examined different phases and compound formations for the samples printed at different heat inputs.

2. MATERIALS AND METHOD

A. Experimental Procedure

The experimental setup utilizes GMAW welding equipment integrated with the MINI CNC 1530 machine. The material deposition rate and the heat source were controlled by the welding machine while the deposition path and its speed were controlled by the CNC machine. The experimental setup of the GMAW-based WAAM system is illustrated in Figure 1.

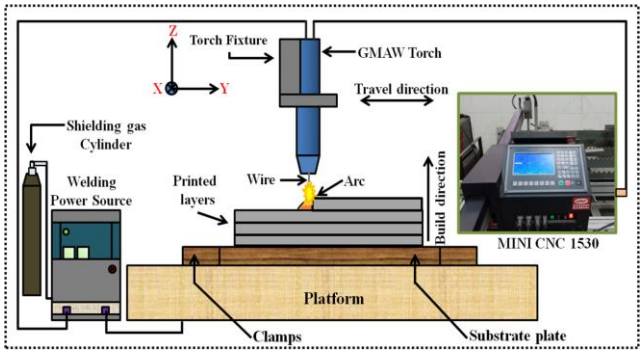

Figure 1: The experimental setup for GMAW-based WAAM technologies

B. Materials Selections

The Stainless steel MIG wire (SS316) of diameter 0.8 mm is used as the feedstock material and the AISI1018 steel plate as the substrate for material deposition. The chemical composition of the filler wire and substrate plate is presented in Table 1. The WAAM process is used to fabricate nine thin straight wall structures of 60mm in length through successive deposition of four layers of metal by varying the heat input in each case.

Table 1
Chemical composition of selected filler wire and support base plate

Elements	C	Cr	Mn	Si	P	Ni	Fe
Substrate (%Wt.)	0.17	0.01	0.8	0.32	0.01	0.004	Bal.
Wire (%Wt.)	0.07	17.0	2.3	0.32	0.04	8.91	Bal.

C. Heat Input and Process Parameters

The WAAM process parameters used during the additive process are listed in Table 2. The stand of distance (SOD) and interlayer dwell time for layers' deposition has been maintained at 10 mm and 60 seconds respectively. The protective gas CO_2 (99.99%) has been used as the shielding medium with a flow rate of 20 L/min maintained during part printing. It provides stability in the process, improvement in the surface finishing quality, and a reduction of the splatters during the process. Furthermore, to investigate the surface topography of the WAAM fabricated surfaces, a square shape structure of 21 layers and a circular shape structure of 15 layers were fabricated using ER70S-6 MIG wire of 0.8 mm diameter considering the optimal process parameters from the previously

published literature (Kumar *et al.*, 2021). In the arc additive process, the thermal input is calculated in each set experiment using Equation (1) (Pépe *et al.*, 2011)

$$H.I\ (J/mm) = \eta \times \frac{U(V)\times I(A)\times 60}{TS(mm/min)} \quad (1)$$

Where HI (J/mm) is the liner heat input of the arc deposition process, η is the thermal efficiency of the GMAW-based WAAM process set to 0.8, U and I are the arc voltage and welding current and TS is the travel speed or deposition speed in (mm/min). It can be seen from Equation 1 that changing the process parameters such as current, voltage, and welding speed can alter the heat input of the fabricated specimen. The influence of heat input on the geometry of the printed wall has been analyzed by changing the arc voltage and current during the WAAM layer deposition process. The dimension of the deposited wall i.e. bead height and bead width has been measured using a digital Vernier Caliper and the average value has been obtained for further study. The average wall height and wall thickness as the process responses have been obtained for each set of the fabricated wall. The final printed four-layered wall by melting a wire using arc energy based on the principle of wire arc additive manufacturing process has been shown in Figure 2. The WAAM process comes with the advantage of a much higher material deposition rate with respect to other metallic additive manufacturing processes (Sydow *et al.*, 2022). In addition to this, a higher working speed allows working with a higher workload and a significantly lesser cost of manufacturing than other AM methods of such category.

Table 2
Experiment Design Matrix for fabricated four-layered wall structure and responses

Samples	Voltage (V)	Current (A)	HI (J/mm)	Avg. wall Height (mm)	Avg. wall Thickness (mm)
1#	14	80	162.90	8.59	9.34
2#	16	85	197.81	8.45	8.83
3#	18	90	235.64	8.51	8.97
4#	20	95	276.36	8.79	9.25
5#	22	100	320.00	8.87	9.58
6#	24	105	366.54	8.95	9.53
7#	26	110	416.00	9.18	10.01
8#	28	115	468.36	9.53	10.15
9#	30	120	523.63	9.61	11.37

Deposition Speed (mm/min): 330

The obtained process response (wall height and width) has been used to study the influence of thermal input on the printed wall geometry. Further, the effect of heat input on the surface quality of the wall has been studied. The surface waviness along the building direction of the printed wall and surface roughness of the final deposited layers has been obtained by using a non-contact optical profilometer and contact-type roughness tester respectively. The fabricated four-layer wall has been sectioned accordingly to investigate the effect of heat input (HI) on the mechanical properties of the deposited wall.

Figure 2: Fabricated WAAM specimens with different Heat Inputs

3. RESULTS AND DISCUSSION

A. Effect of Heat Input on Forming

The printed wall geometry is quantified in terms of average wall height and average wall thickness. The measurement of the height and width of the deposited layered structure is taken by the digital vernier caliper (Model: Mitutoyo 500-196). The effect of heat input on the fabricated wall geometry has been plotted and presented in Figure 3. The results show that the average wall height of the built wall gradually increases with the increase of the heat input to the fabrication process. A similar trend is also followed for the average thickness of the printed four-layer wall structure. The higher thermal input to the process means sufficient heat that can create a better shaped-molten pool layer-upon-layer and provides an improved stabilization effect on the molten pool (Zeng *et al.*, 2021). However, too high heat input results in a higher volume of the molten pool that is expected to spread on the deposited layer deteriorating the geometrical dimension and accuracy. This can be observed from the percentage increases in the average height of sample 9# that gets slightly decreased when compared to sample 8#. On the other hand, to this, lower heat input to the process provides insufficient heat to melt the electrode material in time during layer deposition, and therefore the degree of change in the shape of the molten pool becomes relatively severe. And, the less volume of the melted material during layer deposition reduces the dimension of the printed wall and material deposition efficiency of the WAAM process. The study observed that too high or too low thermal input to the WAAM fabricated specimen is detrimental. Therefore, it is very much critical to adjust and properly select the heat input during the WAAM process as it not only changes the geometry of the printed wall but the existing cooling rate also affects the microstructures and the residual stress within the deposited layers (Jafari *et al.*, 2021).

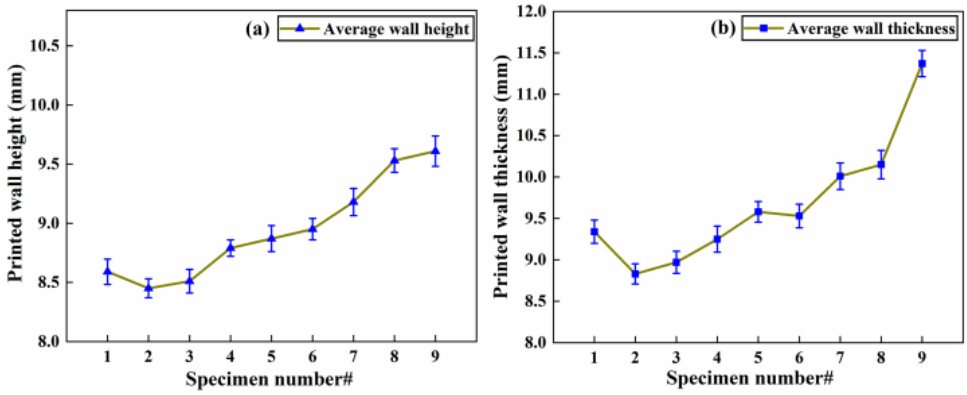

Figure 3: Average height (a) and thickness (b) of the WAAM printed wall specimens with different heat input

B. Effect of Heat Input on Surface Roughness

The quality of the fabricated layered structure is measured in terms of average surface roughness along the deposition direction over the top surface of the final deposited layer. The surface waviness of the built structure along the build direction is analyzed using a non-contact 3D optical profilometer (Model: Zygo, Ametek Newview-9000). However, portable and contact-type surface roughness testers (Model: Mitutoyo SJ-210) were used to obtain the average surface roughness value (Ra) on the top deposited layer of the built structure. The roughness measurement was conducted according to the ISO 4287 standard (Iso, E.N., 1997). The samples before the observation were cleaned using acetone to remove dirt particles. The sampling length and a cut-off length for the contact type roughness tester were taken as 2.4 mm and 0.8 mm respectively. The roughness values were measured at five different locations on the top surface of the final deposited layer for each specimen and the arithmetic means were taken for further analysis. The heat input was found to have a high degree of influence on the surface quality of the fabricated WAAM specimen. There has been a direct dependency of heat input on the surface roughness of the printed wall. Figure 4 shows the bar graph with the error bar scale for the obtained average surface roughness (R_a) on the top surface of the nine WAAM printed specimens against the different heat inputs to their manufacturing process.

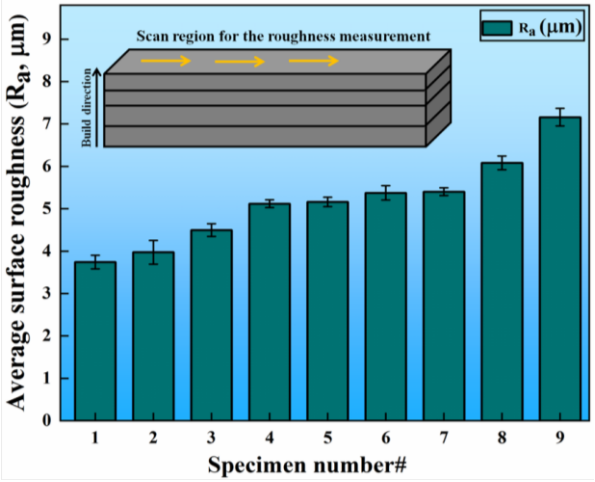

Figure 4: Average surface roughness (R_a) of the final deposited layer of the WAAM printed specimens

The increase in heat input deteriorates the surface quality and increases the surface roughness value on the top surface of the fabricated four-layered wall. It has been observed that the application of high heat input to the WAAM process leads to high heat accumulation and overheating of the deposited material which reduces the surface tension making the molten pool unstable and resulting in a sometimes overflow of the molten pool, arc instability, spattering and the impact of arc force *leads* to a low quality of forming. The surface roughness was found to be reduced with lower heat input but this limited the entire purpose of using WAAM as a low-cost metal additive process. Therefore, to harness the full benefit of WAAM technology, a compromise between the process productivity, surface quality of the printed parts, and mechanical properties needed to be made. Figure 5 shows the 3D surface profile and waviness profile of the printed wall along the building direction of WAAM fabricated specimens at four different heat inputs.

The scan area for the non-contact type optical profilometer is taken as 5.65×3.14 mm. Surface waviness is one of the important parameters to define the quality of WAAM-deposited layers to fabricate different structures. From the literature, it is defined as the maximum peak-to-valley distance measured from the surface profile of the deposited wall. Therefore, the arithmetic mean of the maximum distance between peaks to the valley heights of the deposited layers along the wall-building direction has been obtained using the ImageJ software to quantify the surface waviness of the printed WAAM structure. The values obtained as 1050μm, 910μm, 925μm, and 1169μm for sample 1#, sample 4#, sample 5#, and sample 9#, respectively.

Surface waviness in the WAAM printed walls can also be interpreted as the difference between total wall width (TWW) and effective wall width (EWW). The TWW is the wall thickness directly after the layer deposition while the EWW is the maximum wall width reached after the post-finishing operation of the WAAM printed structure. These observations were used to analyze the effect of different levels of heat input on the built straightness of the WAAM fabricated structure. The build straightness for the multilayer components defines as the deposition of material layer upon layer along the straight-line direction which would be beneficial as the deposited layers closer to

the straight-line result in the least deviation from the wall geometry and therefore require the least post-machining process to correct it. The study found a minimal surface waviness for sample 4# fabricated at 276.36 J/mm. However, the sample fabricated at lower and very high thermal input experienced a greater average value of surface waviness i.e. peak to valley height of the deposited wall along the building direction. The increase in the heat input is responsible for heat accumulation within the printed components that have detrimental effects such as increase in the size of the molten pool and widening of the deposited layer, surface waviness, non-homogenous material along the building direction, and even collapse of possible structure at extremely high heat input. Therefore, well-established management of thermal input can only improve additive manufacturing (AM) part quality and accuracy.

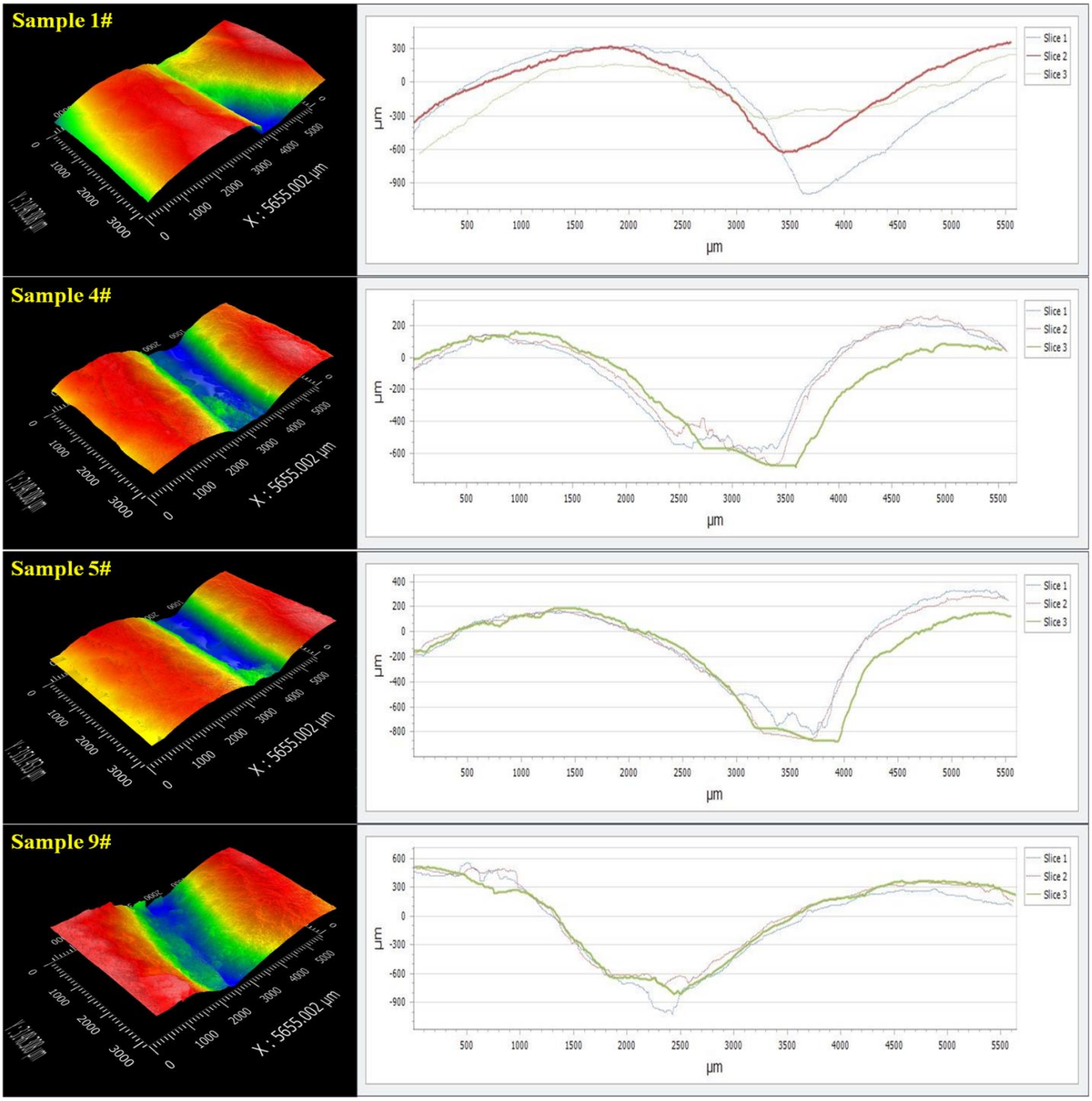

Figure 5: 3D profile image of wall surface and waviness profile of the WAAM-built components at different Heat Inputs

C. Effect of Heat Input on Mechanical Properties

The samples from each printed wall were sectioned and prepared mold using a hot mounting press machine for easy handling of samples. The extracted samples were further polished to remove mild scratches and uneven surfaces. The Vickers micro-hardness test using a repulsive hardness tester (Model: HM220, Mitutoyo Japan) is carried out on the nine extracted samples along the building direction. A load of 0.5 Kgf and a dwell time of 10 seconds were taken as the testing parameter. The hardness tester

uses a pyramidal shape diamond indenter and Quantinet software integrated with the machine for image analyzing and estimating hardness values. The bar graph plotted for the mean hardness value of each tested sample against the heat input to the fabrication process is displayed in Figure 6. The observation shows that the mean hardness value along the building direction decreases with an increase in the heat input to the fabrication process. The high heat input is responsible for increasing the size of dendrite arms spacing due to a lower solidification rate while depositing material layer upon layer thus deteriorating the mechanical properties (Malin, *et al.*, 2020). The slower cooling rate preferentially forms the columnar grain structure in the printed wall also responsible for decreasing the trend of micro-hardness with the increase in heat input. Additionally, it is evident that the interface zones of the printed wall have a higher micro-hardness value compared to it deposited material. Therefore, a suitable inter-pass cooling strategy while depositing material layer by layer can minimize the heat accumulation of the previously deposited material and brings up an almost equivalent solidification rate for each deposited layer. That will result in the least variation in the microstructures along the building direction of the printed. The previous study also found a negative impact of higher heat input on the surface roughness and mechanical properties of the material (Filippov *et al.*, 2021; Chengxun, *et al.*, 2021; Nor Ana, *et al.*, 2021). The use of lower heat input for depositing material layer upon layer along with an application of an inter-layer cooling technique found to be an effective method for grain refinement and reducing mechanical anisotropy (Chengxun, *et al.*, 2021).

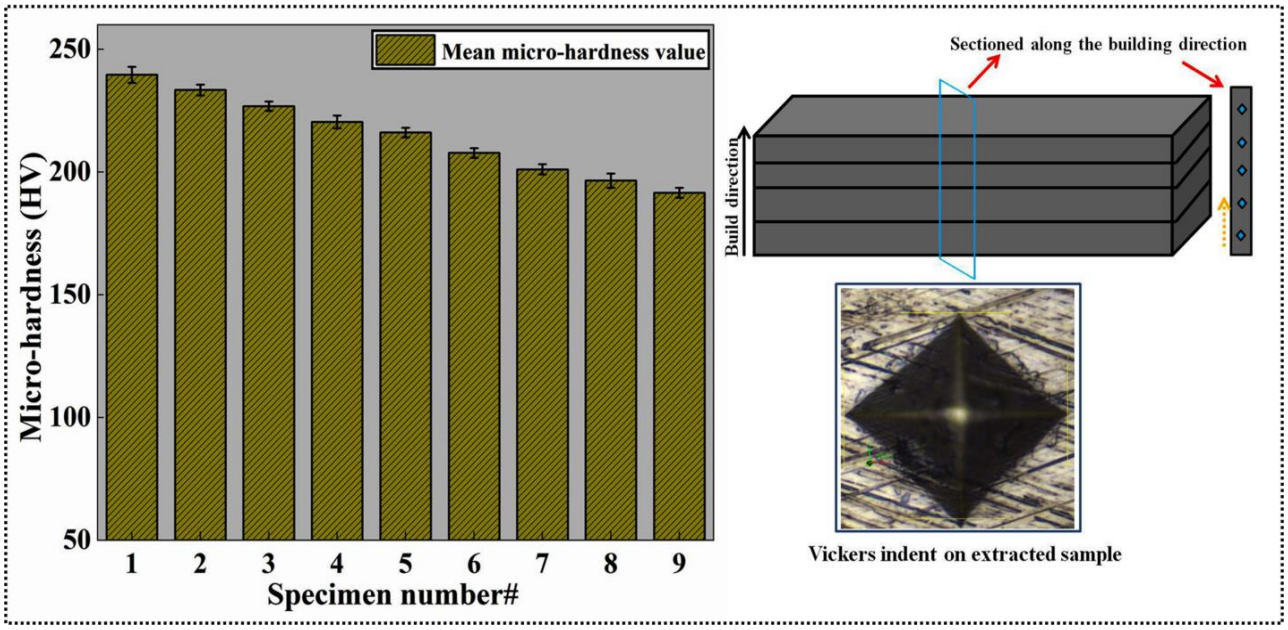

Figure 6: Average hardness value of the WAAM printed wall at different heat inputs

D. Phase Analysis at Different Heat Inputs

X-ray diffraction (XRD) phase analysis has been performed on the selected printed wall samples to investigate and distinguish different phases and compound formation at different levels of heat input. For this analysis, the samples were fabricated at minimum and maximum heat inputs e.g. sample 1# and sample 9#. Besides, two samples were also built at the moderate heat input e.g. sample 4# and sample 5# for the analysis. The samples were tested under the high-resolution (HR) XRD machine (Model- SmartLab studio II) with a radiation source of copper K-α at 40 kV. The diffraction angle (2θ) of 20° to 120°, step size of 0.02°, and a scan speed of 1degree/min are considered as the testing parameters for the generation of XRD peaks. Figure 7 illustrates different peaks and compound formations for samples 1#, 4#, 5#, and 9# printed at different heat levels. The XRD spectra show the presence of intense bcc peaks of residual ferrite (011), (111) (002), (112) for sample 1# along with iron carbides and other solid solution and precipitate responsible for the higher hardness of the tested sample confirming the result of higher hardness value at lower heat input observed under the Vickers micro-hardness test (Garcia-Cabezon *et al.*, 2022). The crystalline phases and compounds having a less intensity peak with a volume fraction lesser than five percent were not been detected in the XRD spectrum of the tested specimen. Furthermore, the sample fabricated at higher heat input shows intense peaks of austenite (111), (002), and (022) in the XRD spectra responsible for the lesser hardness and higher ductility of the fabricated sample (Yadollahi *et al.*, 2017). The peaks also indicate the presence of different oxides of chromium and nickel for sample 9# fabricated at a higher heat input that may be responsible for deteriorating wall quality and impart defects like porosity, and blowholes within the deposited wall built at high thermal input (Keichiro *et al.*, 2009; Miao-Xia *et al.*, 2019). Other than these, identical peaks can be observed for sample 4# and sample 5# printed at moderate heat input with the presence of precipitate and compounds such as chromium-nickel, iron phosphide, manganese nickel, and copper silicon apart from ferrite and austenite phases.

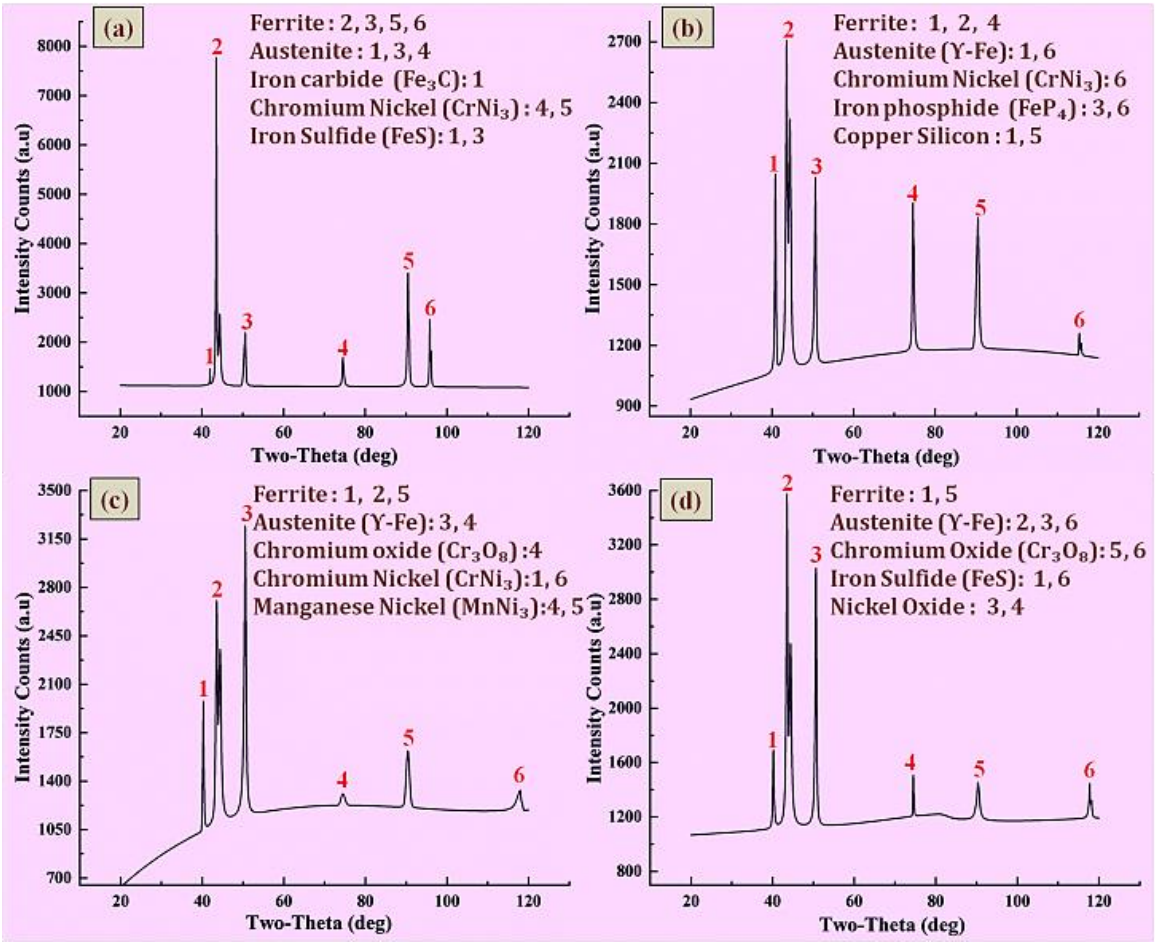

Figure 7: X-ray Diffraction (XRD) Spectra for the WAAM fabricated samples 1# (a), sample 4# (b), sample 5# (c), and sample 9# (d)

E. Surface Topography

The WAAM process when compared to other AM has the advantage of higher material deposition rate that can be reached up to 100% with the right selection of process parameters. However, the surface quality of the deposited parts is always a point of concern to meet the industrial requirement leading to subsequent post-processing of the fabricated parts (Wu *et al.*, 2017). For investigating the surface roughness of two different shapes of WAAM-built structures, 21-layer square shape (A) and 15-layer circular shape (B) components were fabricated using ER70S-6 MIG wire considering the optimal process parameter from the previously published literature (Kumar *et al.*, 2021). Figure 8 displays the three-dimensional (3D) surface profile of the top and bottom regions of the WAAM fabricated component (A) and (B). The 3D non-contact optical profilometer has been used to scan the surface topography of the WAAM-printed walls. The two most important factors used for the evolution of the surface texture of the deposited wall are: Sa (define the arithmetic mean height of the surface) and Sq (define the root mean square height of the surface). The higher value of these two factors for any deposited wall is expected to have a higher roughness value and the surface will be difficult for post-machining due to a rise in its frictional coefficient (Sedlaček *et al.*, 2009). According to the results, the circular shape structure (Component-B) samples possess a lower value of surface roughness with S_a=101.542 µm and Sq = 113.962 µm along the bottom region in comparison to the square shape structure (component-A) with S_a=104.325 µm and S_q=120.597 µm. The scanned areas for the surface profile were chosen away from the bottom and topmost layer of the printed parts where the dimension of the deposited layer is mostly unstable because of the initiation and extinguishing of the arc. The observation from the surface profile along the top and bottom regions of both the components shows a higher roughness value in the top regions of the fabricated component. Thus, the uneven surface appearance and the stair-step effect can be observed in both the printed parts along the building direction with an increase in the number of deposited layers. The higher value of surface waviness generates higher surface roughness on the deposited wall. The surface roughness of the WAAM printed parts depends upon the selected process parameters such as shielding gas, deposition speed, wire feed rate, filler wire diameter, heat input (arc voltage and current supply), and solidification time (Zhijun *et al.*, 2021). For the fabrication of cylindrical shape component B, the welding torch completes one cycle of metal deposition in lesser time around the circular path of diameter (d=22mm) in comparison to square shape wall of dimension (l=30 mm, b=30 mm). Thus, component B gets less time for solidification and so less heat gets accumulated on the deposited layers. This causes reducing

the overflow of the molten pool during the deposition of the next layer which could be a reason for decreases in the surface roughness value in comparison to component A. The WAAM fabricated component-A undergoes post-machining and the uneven surface was machined to reduce the large waviness in the deposited layer. The 2D and 3D surface roughness profiles of the post-machined printed component-A have been shown in Figure 9. The result shows an overall reduction in surface roughness value of the WAAM fabricated component-A with S_a=6.051 µm along the horizontal direction and S_a=9.129 µm along the vertical direction of the deposited layers.

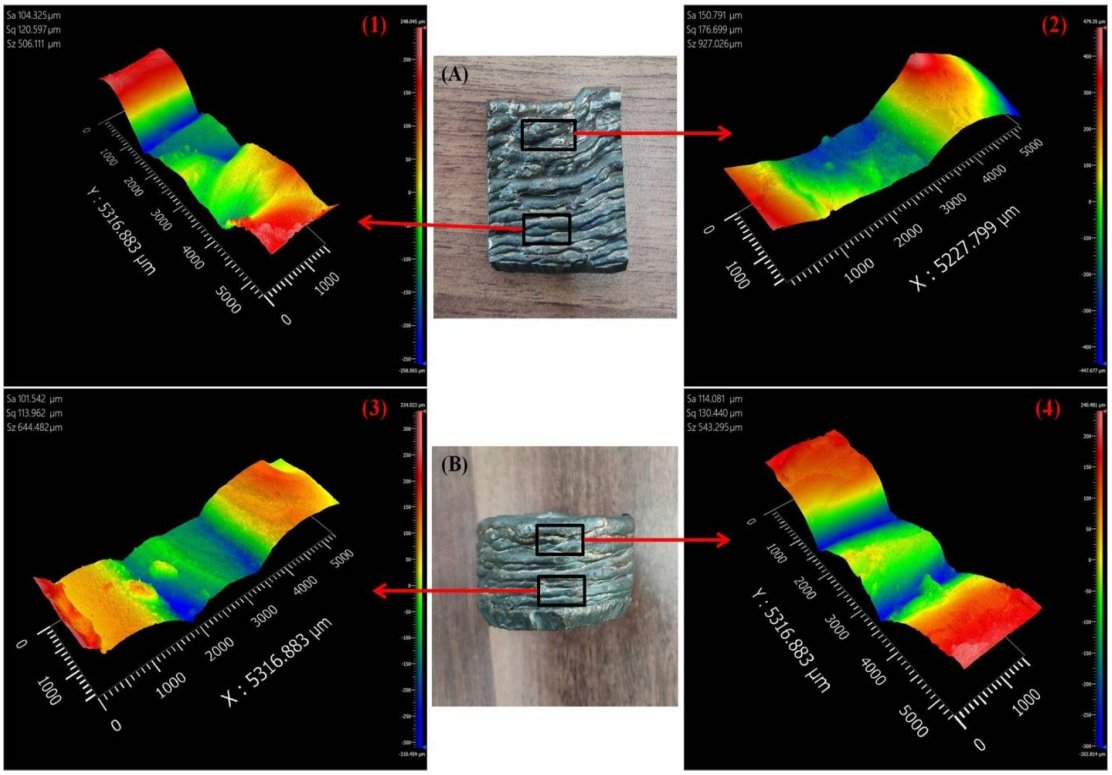

Figure 8: 3D Surface roughness profile of the WAAM fabricated components A and B

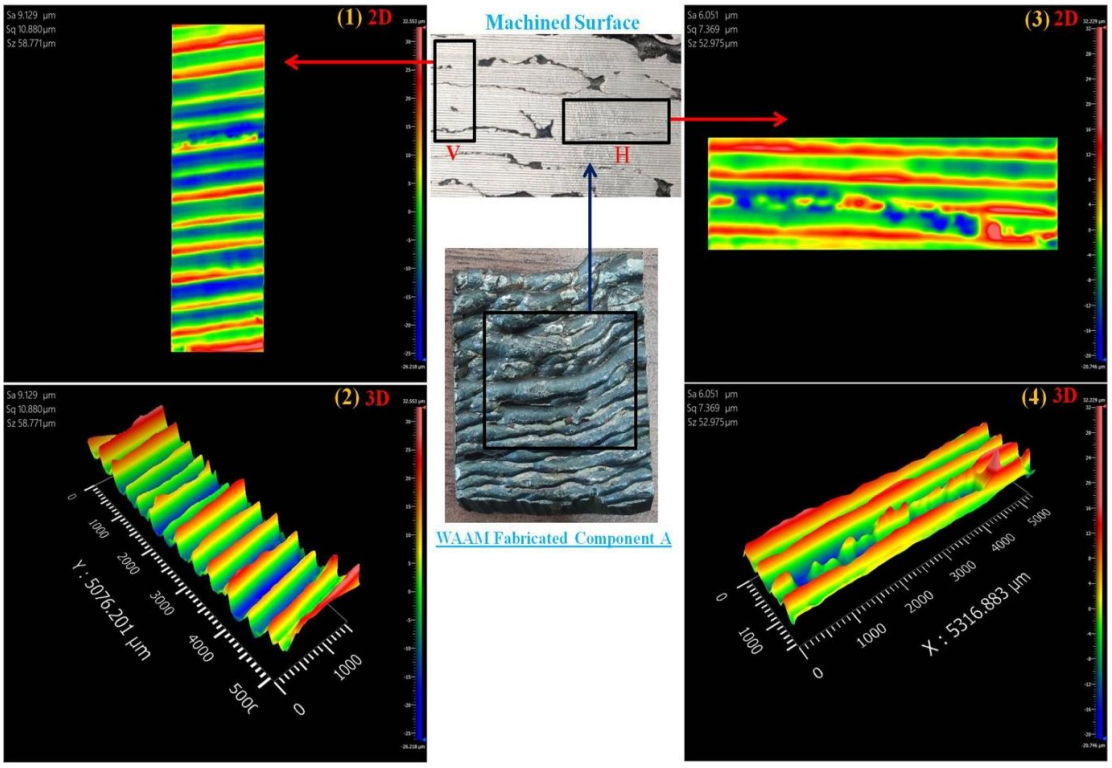

Figure 9: 2D and 3D Surface roughness profile of the post-machined WAAM fabricated Component-A

4. CONCLUSIONS

The critical analysis of surface quality in terms of surface roughness parameters and the effect of thermal input on the surface roughness of the deposited layer, part dimension in terms of wall height and thickness along with mechanical properties of the deposited four-layer wall structure have been concluded as follows.

- Too high or too low thermal input to the WAAM-built specimen is detrimental and therefore fabrication method is required to optimize the heat input to achieve high quality built structure consuming minimal energy with high material deposition efficiency.
- The increased heat input deteriorates the surface quality and surface roughness value on the top surface of the fabricated four-layered wall structure. Also, the surface waviness (peak-to-valley height) largely increased at very high thermal input to the WAAM printed components.
- There has been a negative impact of higher heat input on the mechanical properties of the built structures. The use of optimal heat input for depositing material layer upon layer along with an application of an inter-layer cooling technique concluded to be an effective method for grain refinement and reducing mechanical anisotropy.
- The XRD phase analysis confirms the presence of the intense peak of ferrite along with other carbides and precipitates responsible to impart higher hardness to the WAAM-built structure at lower heat input. Thus support the observation from the micro-hardness testing.
- The surface roughness values along the building direction increase with the number of deposited layers for both the WAAM fabricated component-A (square shape structure) and B (circular shape structure). The cylindrical shape structure was found to have a lesser roughness value when compared to the square-shaped structure.

The study investigates the influence of equivalent heat inputs on the formability, surface quality, and mechanical properties of the WAAM fabricated steel structures. However, an in-depth study based on the impact of heat input on the grain morphology, and tribological performance along different orientations needs further investigation. Also, different cooling strategies to mitigate the excessive heat accumulation and anisotropic behaviour of the WAAM-built structures are some other future scope of the research work.

ACKNOWLEDGMENTS

This work was supported by the Science and Engineering Research Board (DST-SERB), Govt. of India under grant numbers [SR/FST/ET-II/2018/222(C)] & [EEQ/2021/000l84].

REFERENCES

Dirisu, P., Supriyo, G., Martina, F., Xu, X. and Williams, S., (2020). Wire plus arc additive manufactured functional steel surfaces enhanced by rolling. *International Journal of Fatigue*, *130*, p.105237. DOI: https://doi.org/10.1016/j.ijfatigue.2019.105237

Filippov, A., Shamarin, N., Moskvichev, E., Savchenko, N., Kolubaev, E., Khoroshko, E. and Tarasov, S., (2021**)**. Heat Input Effect on Microstructure and Mechanical Properties of Electron Beam Additive Manufactured (EBAM) Cu-7.5 wt.% Al Bronze. *Materials*, *14*(22), p.6948. DOI: https://doi.org/10.3390/ma14226948

Garcia-Cabezon, C., Castro-Sastre, M.A., Fernandez-Abia, A.I., Rodriguez-Mendez, M.L. and Martin-Pedrosa, F., (2022**)**. Microstructure–hardness–corrosion performance of 17–4 precipitation hardening stainless steels processed by selective laser melting in comparison with commercial alloy. *Metals and Materials International*, *28*(11), pp.2652-2667) DOI: https://doi.org/10.1007/s12540-021-01155-8

Gisario, A., Kazarian, M., Martina, F. and Mehrpouya, M., (2019**)**. Metal additive manufacturing in the commercial aviation industry: A review. *Journal of Manufacturing Systems*, *53*, pp.124-149. DOI: https://doi.org/10.1016/j.jmsy.2019.08.005

Gudur, S., Nagallapati, V., Pawar, S., Muvvala, G. and Simhambhatla, S., (2021**)**. A study on the effect of substrate heating and cooling on bead geometry in wire arc additive manufacturing and its correlation with cooling rate. *Materials Today: Proceedings*, *41*, pp.431-436. DOI: https://doi.org/10.1016/j.matpr.2020.10.071

Guo, Y., Quan, G., Celikin, M., Ren, L., Zhan, Y., Fan, L. and Pan, H., (2022**)**. Effect of heat treatment on the microstructure and mechanical properties of AZ80M magnesium alloy fabricated by wire arc additive manufacturing. *Journal of Magnesium and Alloys*, *10*(7), pp.1930-1940. DOI: https://doi.org/10.1016/j.jma.2021.04.006

Hönnige, J.R., Colegrove, P.A., Ahmad, B., Fitzpatrick, M.E., Ganguly, S., Lee, T.L. and Williams, S.W., (2018**)**. Residual stress and texture control in Ti-6Al-4V wire+ arc additively manufactured intersections by stress relief and rolling. *Materials & Design*, *150*, pp.193-205. DOI: https://doi.org/10.1016/j.matdes.2018.03.065

International Organization for Standardization, (1996**)**. Geometrical Product Specifications (GPS)--surface Texture: Profile Method--rules and Procedures for the Assessment of Surface Texture. ISO.

Jafari, D., Vaneker, T.H. and Gibson, I., (2021**)**. Wire and arc additive manufacturing: Opportunities and challenges to control the quality and accuracy of manufactured parts. *Materials & Design*, *202*, p.109471. DOI: https://doi.org/10.1016/j.matdes.2021.109471

Kumar, V., Mandal, A., Das, A.K. and Kumar, S., (2021**)**. Parametric study and characterization of wire arc additive manufactured steel structures. *The International Journal of Advanced Manufacturing Technology*, *115*(5-6), pp.1723-1733. DOI: https://doi.org/10.1007/s00170-021-07261-6

Lervåg, M., Sørensen, C., Robertstad, A., Brønstad, B.M., Nyhus, B., Eriksson, M., Aune, R., Ren, X., Akselsen, O. M., and Bunaziv, I., (2020**)**. Additive manufacturing with superduplex stainless steel wire by cmt process. *Metals*, *10*(2), p.272. DOI: https://doi.org/10.3390/met10020272

Nagamatsu, H., Sasahara, H., Mitsutake, Y. and Hamamoto, T., (2020**)**. Development of a cooperative system for wire and arc additive manufacturing and machining. *Additive Manufacturing*, *31*, p.100896. DOI: https://doi.org/10.1016/j.addma.2019.100896

Ohsawa, K., Hayashi, Y., Hasunuma, R. and Yamabe, K., (2009**)**, November. Roughness increase on surface and interface of SiO2 grown on atomically flat Si (111) terrace. In *Journal of Physics: Conference Series* (Vol. 191, No. 1, p. 012031).

IOP Publishing. DOI: 10.1088/1742-6596/191/1/012031

Pépe, N., Egerland, S., Colegrove, P.A., Yapp, D., Leonhartsberger, A. and Scotti, A., (2011**)**. Measuring the process efficiency of controlled gas metal arc welding processes. *Science and Technology of Welding and Joining*, *16*(5), pp.412-417. DOI: https://doi.org/10.1179/1362171810Y.0000000029

Qiu, Z., Dong, B., Wu, B., Wang, Z., Carpenter, K., Wu, T., Zhang, J., Wexler, D., Zhu, H. and Li, H., (2021**)**. Tailoring the surface finish, dendritic microstructure and mechanical properties of wire arc additively manufactured Hastelloy C276 alloy by magnetic arc oscillation. *Additive Manufacturing*, *48*, p.102397. DOI: https://doi.org/10.1016/j.addma.2021.102397

Qi, Z., Cong, B., Qi, B., Zhao, G. and Ding, J., (2018**)**. Properties of wire+ arc additively manufactured 2024 aluminum alloy with different solution treatment temperature. *Materials Letters*, *230*, pp.275-278. DOI: https://doi.org/10.1016/j.matlet.2018.07.144

Rosli, N.A., Alkahari, M.R., bin Abdollah, M.F., Maidin, S., Ramli, F.R. and Herawan, S.G., (2021**)**. Review on effect of heat input for wire arc additive manufacturing process. *Journal of Materials Research and Technology*, *11*, pp.2127-2145. DOI: https://doi.org/10.1016/j.jmrt.2021.02.002

Sedlaček, M., Podgornik, B. and Vižintin, J., (2009**)**. Influence of surface preparation on roughness parameters, friction and wear. *Wear*, *266*(3-4), pp.482-487. DOI: https://doi.org/10.1016/j.wear.2008.04.017

Sydow, B., Jhanji, A., Hälsig, A., Buhl, J. and Härtel, S., (2022**)**. The Benefit of the Process Combination of Wire Arc Additive Manufacturing (WAAM) and Forming—A Numerical and Experimental Study. *Metals*, *12*(6), p.988. DOI: https://doi.org/10.3390/met12060988

Wang, S., Gu, H., Wang, W., Li, C., Ren, L., Wang, Z., Zhai, Y. and Ma, P., (2020**)**. The influence of heat input on the microstructure and properties of wire-arc-additive-manufactured Al-Cu-Sn alloy deposits. *Metals*, *10*(1), p.79. DOI: https://doi.org/10.3390/met10010079

Wu, Q., Lu, J., Liu, C., Fan, H., Shi, X., Fu, J. and Ma, S., (2017**)**. Effect of molten pool size on microstructure and tensile properties of wire arc additive manufacturing of Ti-6Al-4V alloy. *Materials*, *10*(7), p.749. DOI: https://doi.org/10.3390/ma10070749

Xie, Miao-Xia, *et al.*, (2019). "Effect of heat input on porosity defects in a fiber laser welded socket-joint made of powder metallurgy molybdenum alloy." *Materials* 12.9: 1433. DOI: https://doi.org/10.3390/ma12091433

Xie, M.X., Li, Y.X., Shang, X.T., Wang, X.W. and Pei, J.Y., (2019**)**. Effect of heat input on porosity defects in a fiber laser welded socket-joint made of powder metallurgy molybdenum alloy. *Materials*, *12*(9), p.1433. DOI: https://doi.org/10.1016/j.jmatprotec.2017.09.020

Yadollahi, A., Shamsaei, N., Thompson, S.M., Elwany, A. and Bian, L., (2017**)**. Effects of building orientation and heat treatment on fatigue behavior of selective laser melted 17-4 PH stainless steel. *International Journal of Fatigue*, *94*, pp.218-235. DOI: https://doi.org/10.1016/j.ijfatigue.2016.03.014

Zeng, J., Nie, W. and Li, X., (2021). The influence of heat input on the surface quality of wire and arc additive manufacturing. *Applied Sciences*, *11*(21), p.10201. DOI: https://doi.org/10.3390/app112110201

Zeng, Y., Wang, X., Qin, X., Hua, L. and Xu, M., (2021). Laser Ultrasonic inspection of a Wire+ Arc Additive Manufactured (WAAM) sample with artificial defects. *Ultrasonics*, *110*, p.106273. DOI: https://doi.org/10.1016/j.ultras.2020.106273

Zhang, C., Qiu, Z., Zhu, H., Wang, Z., Muránsky, O., Ionescu, M., Pan, Z., Xi, J. and Li, H., (2022**)**. On the effect of heat input and interpass temperature on the performance of inconel 625 alloy deposited using wire arc additive manufacturing–cold metal transfer process. *Metals*, *12*(1), p.46. DOI: https://doi.org/10.3390/met12010046

Zhou, Y., Lin, X., Kang, N., Huang, W., Wang, J. and Wang, Z., (2020). Influence of travel speed on microstructure and mechanical properties of wire+ arc additively manufactured 2219 aluminum alloy. *Journal of Materials Science & Technology*, *37*, pp.143-153. DOI: https://doi.org/10.1016/j.jmst.2019.06.016